

Chapter 5

Electrochemical Detection of MSG

5.1 Introduction

Monosodium L-glutamate (MSG) is a naturally occurring non-essential amino acid [185]. MSG has been utilized as a taste enhancer in the food industry. However, Food and Drug Administration (FDA) has acknowledged that people might suffer adverse effects with symptoms like sweating, weakness, nausea, headache, bronchospasm, rapid heartbeat, chest pain, and drowsiness to the excessive use of MSG [186]. Several research reports have also shown side effects of MSG on the human body as Chinese restaurant syndrome [187], Parkinson's disease [188], Alzheimer's disease [189], schizophrenia [190], depression [191], and birth deformity in posterity among pregnant women [192]. Since then, several regulatory bodies have considered these findings to set a range of MSG concentrations in food products [193], [194]. Despite this, the food industry often uses MSG beyond standard limits to augment its product's taste.

A range of analytical techniques in the laboratory, such as chromatography [195], surface plasmon resonance [196], chemiluminescence [197], spectrophotometry, fluorescence [198], and capillary electrophoresis are used for MSG detection [199]. Several studies have also described the use of electrochemical detection of MSG, which provides advantages over conventional methodologies [200]–[207]. Enzymatic-based electrochemical biosensors have been extensively used but have a low detection range as their limitation [208]–[214]. A relative comparison of different biosensors for detecting MSG is summarized in **table 5.1**.

Table 5.1: Relative comparison of different types of biosensors for the detection of MSG

| Immobilization Technique | Ref | Lowest Detection | Sensitivity | Linear Range | Response Time |
|---|------------|-------------------------|---|---------------------------|----------------------|
| Au@MoS ₂ /chitosan electrode using monoclonal antibody | [93] | 0.05 μM | NA | 0.05 to 200 μM | NA |
| Poly-carbamoylsulphonate hydrogel mixed with glutamate oxidase | [74] | 1.01 μM | 1.94 nA/ μM | 100 - 5000 μM | NS |
| Titania and ceria and nanoparticles for glutamate detection in hypoxic environments | [75] | 0.594 μM | 0.79 nA/ μM | 5 – 50 μM | ~5 |
| Biosensor for L-Glutamic Acid using Glutamate Oxidase and Effective Rejection of Interferences | [76] | 0.27 μM | 3.8 nA $\text{cm}^{-2} \text{mM}^{-1} \text{L}$ | 0 - 100 μM | <10s |
| Polyion complex-bilayer membrane | [77] | 0.2 nM | 1.85 nA/ μM | 3 – 500 μM | NS |
| Carboxylated MWCNT/gold nanoparticles/chitosan composite film modified Au electrode | [79] | 1.6 μM | 155 nA/ $\mu\text{M}/\text{cm}^2$ | 5 – 500 μM | 2s |
| Pt nanoparticles modified gold nanowire array electrode | [80] | 14 μM | 194.6 $\mu\text{A} \text{mM}^{-1} \text{cm}^{-2}$ | 200 - 800 μM | 4.8s |
| Palladium-deposited screen-printed carbon electrode | [81] | 0.05 μM | 12.8 nA/ μM | 0.05 - 100 μM | 30 – 50 s |
| Cross-linking with Glutaraldehyde and BSA as a spacing agent | [21 5] | N/A | NS | NS | 120s |
| Polypyrrole nanoparticles/polyaniline-modified Au electrode | [21 6] | 0.1 nM | 533 nA/ $\mu\text{M}/\text{cm}^2$ | 0.02 - 400 μM | 3s |
| A composite of carbon paste, octadecyl amine, and mitochondria fraction, onto the working electrode | [84] | 100 μM | 0.189 $\mu\text{A}/\text{mM}$ | 0.4 - 10 mM | N/A |
| layers-by-layer assembly of glutamate dehydrogenase and Pt-PAMAM | [85] | 100 μM | 433 $\mu\text{A}/\text{mM}^{-1} \text{cm}^2$ | 0.2 - 250 μM | 3s |

| | | | | | |
|--|------|-------------|--|--------------------|-----------|
| Carbon paste mixed with lyophilized enzyme and coenzyme, packed into the well of a working electrode | [86] | 3.8 μ M | 4.6 $\times 10^5$ nA l mol ⁻¹ | 5 - 78 μ M | 120s |
| GLDH based CNT-CHIT-MDB modified GC electrode | [87] | 2 μ M | 0.71 nA/ μ M | 25 - 100 μ M | NS |
| Immobilization of GLDH with Chitosan, drop coated onto a screen-printed carbon electrode | [89] | 1.5 μ M | 0.44 nA/ μ M | 12.5 - 150 μ M | 2s |
| Immobilization of NAD ⁺ and GLDH by using a mixture of CHIT/MWCNT/MB drop coated onto the screen-printed carbon electrode | [90] | 3 μ M | 0.39 nA/ μ M | 7.5 - 105 μ M | 20 – 30 s |

Other challenges in developing electrochemical biosensors are associated with the effective immobilization of receptor molecules, minimizing charge transportation resistance, high selectivity, and reproducibility.

5.2 Materials & Instrumentation

L-glutamic acid monosodium salt hydrate 99% (MSG), N-(3 dimethylamino propyl)-N'-ethyl carbodiimide hydrochloride (EDC), N-hydroxysuccinimide (NHS), sodium phosphate monobasic (NaH₂PO₄), disodium hydrogen phosphate (Na₂HPO₄), potassium chloride (KCl), sodium hydroxide (NaOH) and potassium ferrocyanide [K₄Fe(CN)₆] were purchased from Sigma-Aldrich. Bovine Serum Albumin (BSA) was procured from AcRos. Rabbit Anti-glutamate antibody was obtained from Merck Millipore, USA. Deionized (DI) water from a Millipore system (~18.2 M Ω cm) was used to prepare experimental solutions.

Electrochemical measurements were performed using GAMRY Reference 3000, potentiostat/ galvanostat/ZRA, USA.

5.3 Electrochemical Detection of MSG by GNP-chitosan Nanocomposite.

A composite of gold nanoparticles (GNP) with chitosan (CS) was synthesized through in situ reduction process enabling uniform distribution of the metal-polymer network. The composite material was coated on a glassy carbon electrode (GCE) to enhance functionalization capability and charge transportation. The coating of GNP incorporated CS on GCE enhanced current in cyclic voltammetry and differential pulse voltammetry (DPV) measurements. This electrode was functionalized with NHS-EDC to attain a higher degree of immobilization of rabbit anti-glutamate antibodies. Monosodium L-glutamate (MSG) detection in the electrolyte was quantified by measuring a decrease in the peak current of DPV due to their interaction with antibodies at the surface of the working electrode. Electrochemical impedance spectroscopy (EIS) measurement also showed a relative increase in impedance with an increase in MSG concentration. The biosensor showed a linear response from 100 pM to 1 μ M with a detection sensitivity of the order $\sim 102 \mu\text{A/nM}$.

5.3.1 Preparation of Anti-Glutamate Monoclonal Antibody Functionalized Immunosensor

The glassy carbon electrode (GCE) was cleaned with 0.3 μm and 0.05 μm micro polish alumina (Buehler, USA), followed by 30 min sonication in ethanol and water to obtain a clean and impurity-free surface. After that, the GCE was dried at room temperature. 10 μL of CS-GNP nanocomposite was drop cast onto the clean surface of 3 mm GCE. Modified CS-GNP GCE was dried at room temperature for 48 h. EDC-NHS coupling reaction was used to generate amine groups over the CS-GNP coatings on the surface of GCE [213]. 100 mM NHS and 400 mM EDC were prepared as stock solutions in 100 mM PBS (pH 7.2) and

stored at 4°C. Further EDC-NHS mixture was prepared by mixing NHS and EDC in a 1:1 ratio [218], [219]. 10 μL of EDC-NHS mixture was cast onto the modified GCE surface and

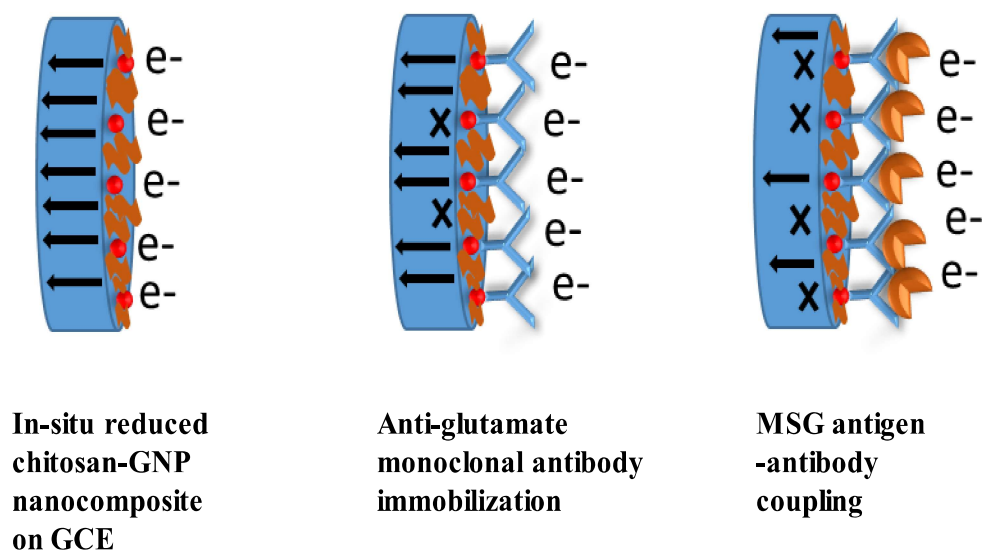


Figure 5.1: Schematic diagram for fabrication of working electrode platforms.

dried for two h. After drying, 5 μL of anti-glutamate monoclonal antibody (1:100 dilution in PBS) was immobilized onto the functionalized GCE and kept for 12 h at 4°C. This developed immunosensor (CS-GNP-AB) was rinsed thoroughly with PBS to remove the unbound molecules. The schematic representation of the fabricated immunosensor is shown in **Figure 5.1**.

5.3.2 Electrochemical Characteristics

An electrochemical immunosensor for MSG detection was set up using a three-electrode system. GCE as the working electrode, platinum (Pt) wire as a counter, and Ag/AgCl (3.0M KCl) as the reference electrode was used. The CV was recorded in 100 mM PBS (pH 7.2) containing 5 mM $\text{K}_4[\text{Fe}(\text{CN})_6]$ and 0.1 M KCl in the potential window of -0.3 V to +0.9 V with a scan rate of 15 mVs^{-1} . The current variation of the immunosensor was recorded with

the change in MSG concentration. The CV results of GCE, chitosan-coated GCE (CS), the composite of CS-

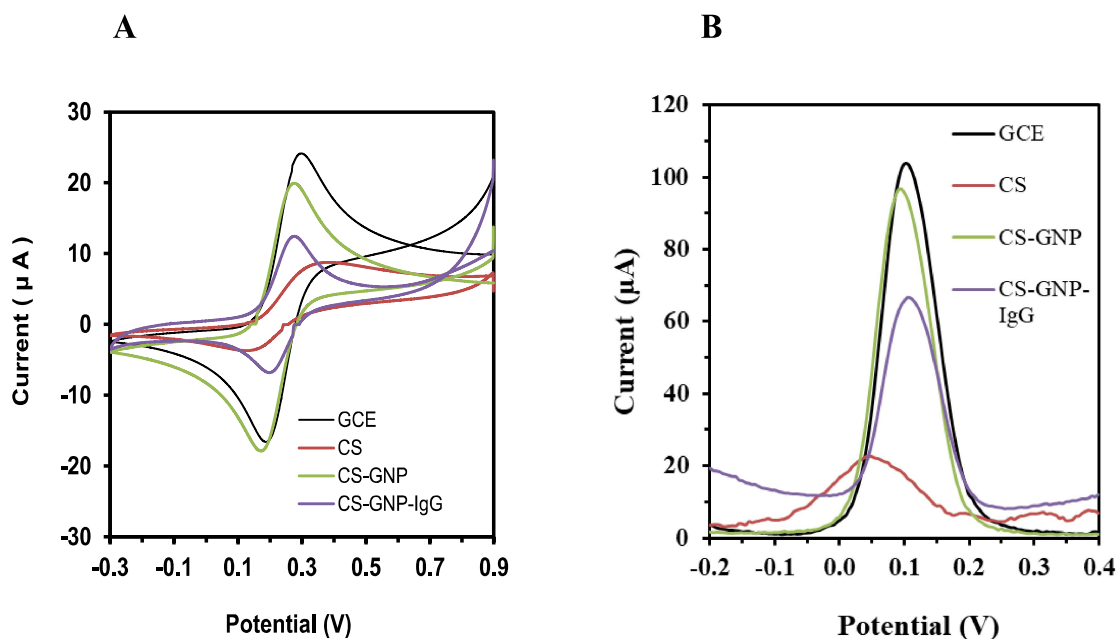


Figure 5.2: (A) CV and (B) DPV of different working electrodes. Glassy carbon electrode (GCE), chitosan (CS), chitosan -gold nanoparticles (CS-GNP), Rabbit anti-glutamate antibodies functionalized chitosan – gold nanoparticles (CS-GNP-AB).

GNP-coated GCE (CS-GNP) and antibody immobilized on EDC-NHS functionalized on CS-GNP composite coatings on GCE (CS-GNP-AB) are shown in **Figure 5.2 A**.

The peak currents associated with anodic (E_{pa}) and cathodic (E_{pc}) potentials in the CV were measured for each step during the development of the working electrode for the relative assessment of charge transportation at the surface. The anodic current (I_{pa}) and cathodic current (I_{pc}) were decreased from $\sim 24 \mu\text{A}$ to $\sim 9 \mu\text{A}$ and from $\sim -17 \mu\text{A}$ to $\sim -4 \mu\text{A}$, respectively, after coating with CS on the GCE due to the non-conductive nature of chitosan. The coating of CS-GNP composite materials on GCE enhanced both I_{pa} and I_{pc} from $\sim 9 \mu\text{A}$ to $\sim 20 \mu\text{A}$ and from $\sim -4 \mu\text{A}$ to $\sim -17.9 \mu\text{A}$, respectively.

Noticeable change in anodic and cathodic peak potential was also observed in the CV response of CS and CS-GNP composite coatings on GCE. Furthermore, immobilization with rabbit anti-glutamate antibodies on the CS-GNP network showed a decrease in I_{pa} and I_{pc} from $19.9 \mu\text{A}$ to $12.43 \mu\text{A}$ and $-17.9 \mu\text{A}$

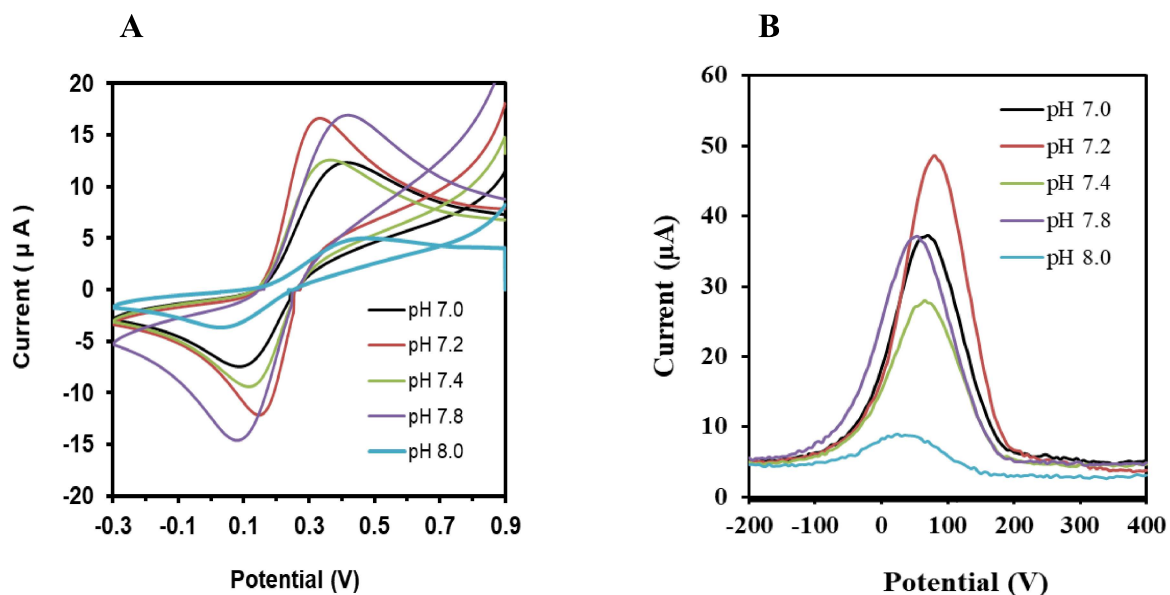


Figure 5.3: (A) CV and (B) DPV response of CS-GNP-AB working electrode at various pH levels.

to $-6.8 \mu\text{A}$, respectively, as shown in **Figure 5.2 A**. The anodic and cathodic peak potential was also slightly shifted after the immobilization of antibodies on CS-GNP-coated GCE. **Figure 5.2 B** shows that DPV responses of GCE, CS, CS-GNP, and CS-GNP-AB biosensor platforms were recorded in the same electrolyte. DPV peak current (I_p) was decreased from $\sim 104 \mu\text{A}$ to $\sim 23 \mu\text{A}$ after CS coating on GCE. The I_p was significantly enhanced (from $\sim 23 \mu\text{A}$ to $\sim 97 \mu\text{A}$) by the coating of the CS-GNP composite. Rabbit anti-glutamate antibodies functionalized CS-GNP platforms resulting in I_p value of $\sim 67 \mu\text{A}$.

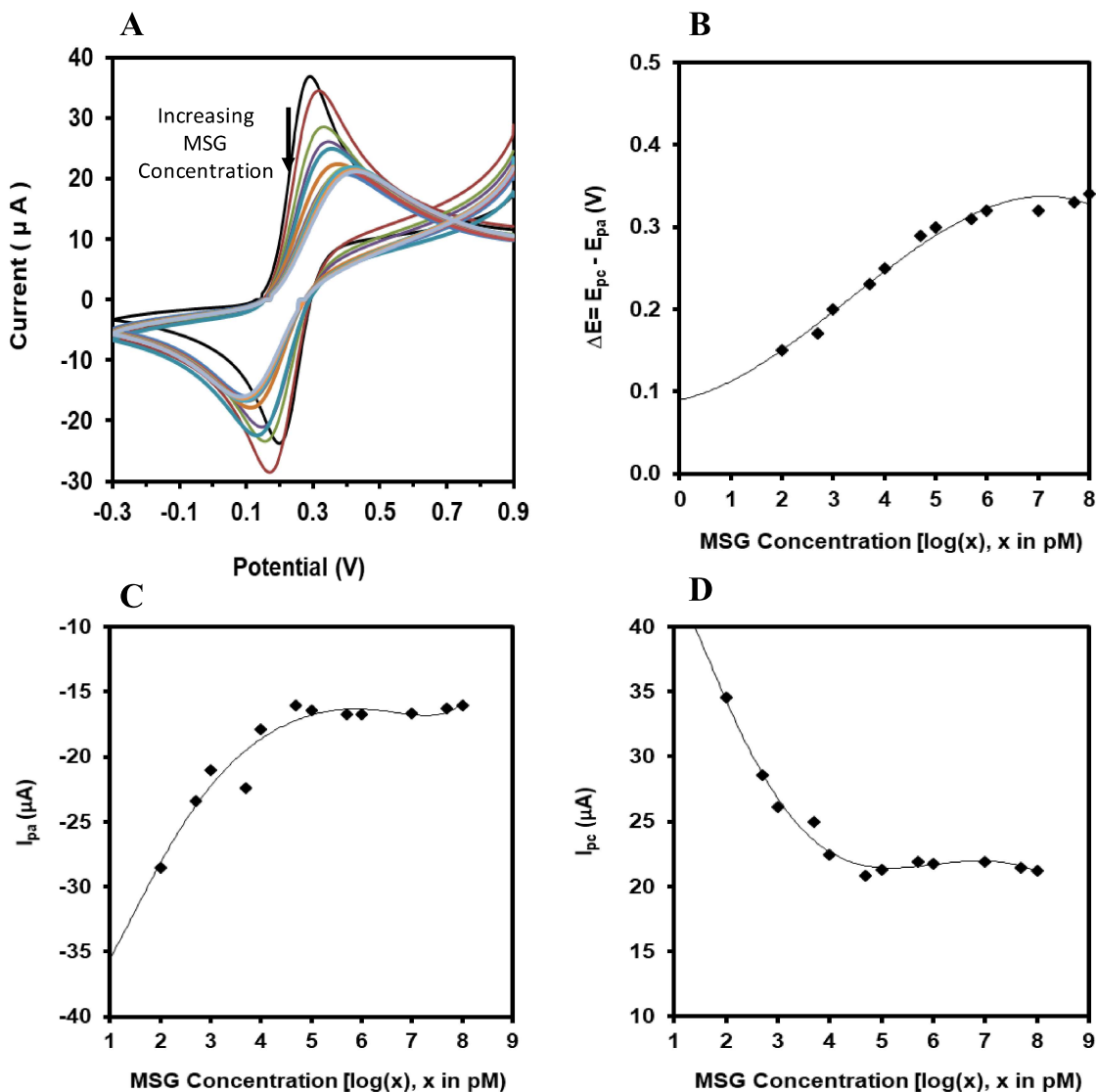


Figure 5.4: (A) CV response of CS-GNP-AB working electrode with different concentrations of MSG. Relative change in (B) oxidation and reduction peak potential, (C) Anodic peak current, and (D) cathodic peak current with MSG concentrations. The result was obtained for $n=4$ substrates with an average error of 8% to 13%.

The electrochemical response of biosensor working electrodes was examined at various pH conditions varying from 7.0 to 8.0. **Figure 5.3 A** and **B** show CV and DPV response with the change in pH of electrolyte solution, which shows a vital role in the electrochemical detection process. This was expected due to varying pH variations in the ionic concentration of

electrolytes. The result showed a similar pattern in a change of anodic and cathodic peak current in CV with the change in peak current of DPV response.

However, the electrochemical response at pH values shows variations in current conduction, which are inconsistent with a gradual increase in the pH. At this stage, the underlying physical process is not well understood. The results showed the highest current conduction at pH 7.2, resembling the best efficacy and effectiveness of antibody-functionalized biosensor

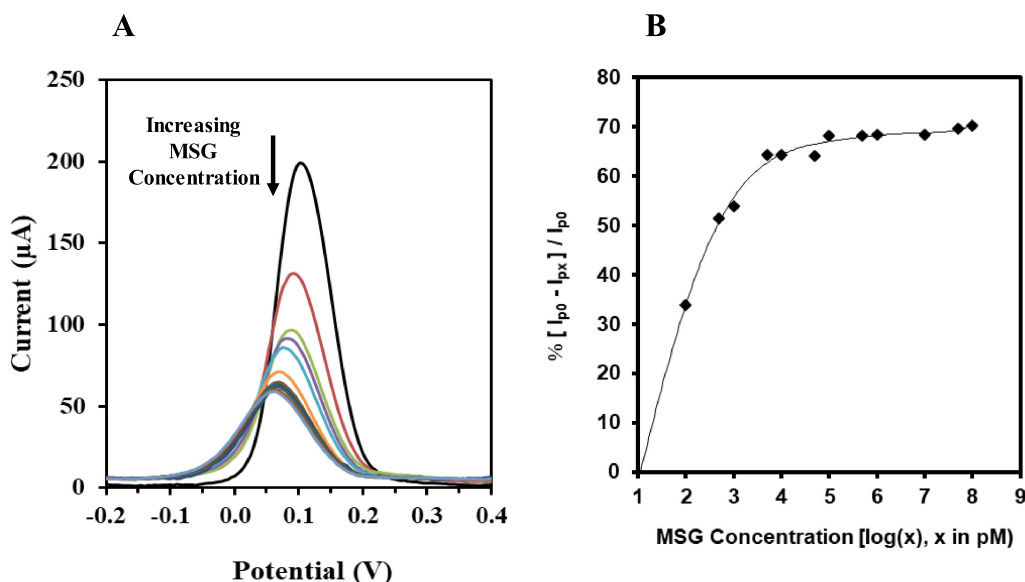


Figure 5.5: (A) DPV response of CS-GNP-AB working electrode with different concentrations of MSG. (B) Relative change in % peak current with MSG concentrations. The result was obtained for $n=4$ substrates with an average error of 8% to 13%.

working electrodes. In further experiments, intending to obtain higher sensitivity of the developed biosensor, we have adopted a working pH condition of 7.2 instead of a standard physiological condition of 7.4 as reported in many studies [60]. The CV response of the antibody-immobilized working electrode was recorded at varying concentrations of MSG from 0.1 nM to 100 μM; the results are shown in **Figure 5.4 A**. The interaction of MSG with antibodies at the surface of the working electrode showed a shift in both anodic and cathodic

peak potential. The difference between anodic and cathodic peak potential ($\Delta E = E_{pc} - E_{pa}$) was calculated at different concentrations of MSG. **Figure 5.4 B** initially shows a linear increase in ΔE with an increase in MSG concentration and reaches saturation at a higher concentration of MSG in the electrolyte. I_{pa} and I_{pc} current responses of the working electrode from **Figure 5.4 A** were measured and compared with the CV response of the electrode without the addition of MSG in the electrolyte. **Figure 5.4 C** shows a decrease in anodic peak current from $\sim 37 \mu\text{A}$ to $\sim 22 \mu\text{A}$ with an increase in MSG concentration from 0.1 nM to 100 μM , respectively. Contrary, **Figure 5.4 D** shows a change in cathodic peak current from $\sim -24 \mu\text{A}$ to $\sim -16 \mu\text{A}$. However, a further rise in MSG concentration did not significantly change the current response.

DPV response of the biosensor working electrode was recorded with various concentrations of MSG, and the results are shown in **Figure 5.5 A**. The observation revealed that the peak current gradually decreased with an increase in the MSG concentration. This may be due to the formation of anti-glutamate antibodies and L-glutamate antigen complex, which plays an important role in the selective detection of MSG. This complex system creates a diffusion layer that blocks the transfer of ions between the solution and electrode surface. As a result, active sites for electron transfer were reduced, and the working electrode platform's conductivity was decreased with an increase in MSG concentration. **Figure 5.5 B** shows a decrease in peak current with increased MSG concentration during DPV measurement. The detection sensitivity was calculated and found to be 10^5 A/M for the range of $<1 \text{ nM}$ and $6 \times 10^2 \text{ A/M}$ for the concentration of $\text{MSG} > 1 \text{ nM}$ in the solution.

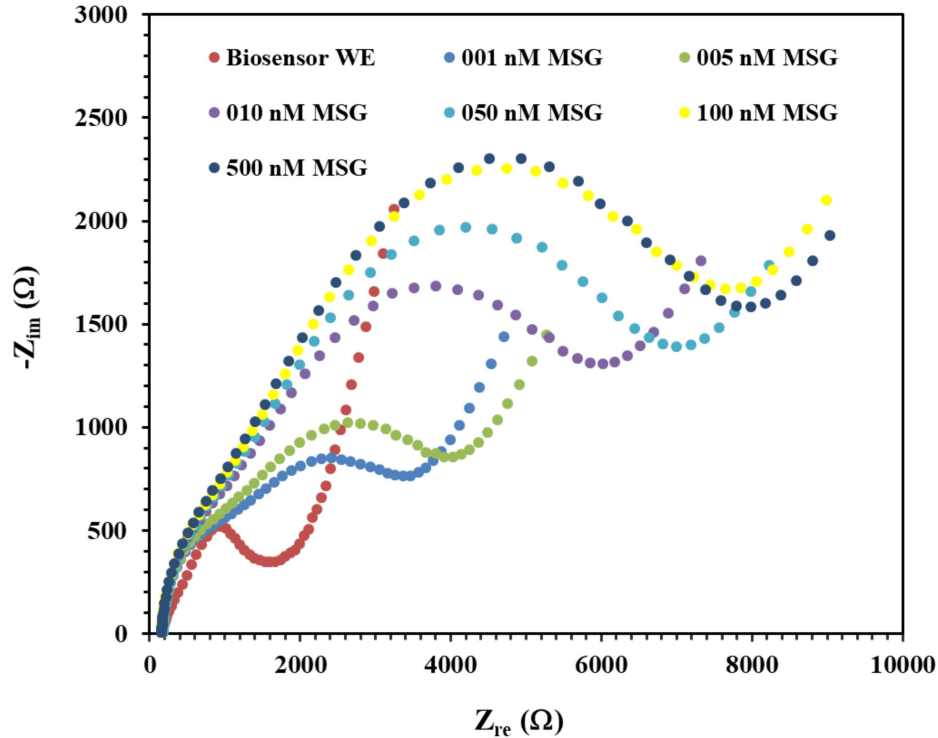


Figure 5.6: Nyquist plots at various MSG concentrations (from 1 nM to 500 nM) in electrolytes obtained from antibodies immobilized working electrode (biosensors WE) for the impedance obtained between 1 MHz and 0.1 Hz frequency variation.

Electrochemical impedance spectroscopy (EIS) was performed to further confirm the interaction of MSG with antibodies at the composite surface, which led to a reduction in peak current as observed in DPV measurements. **Figure 5.6** showed the EIS spectra of working biosensor electrodes and indicated the lowest impedance values. However, the addition of MSG in electrolytes showed a gradual increase in the impedance. The impedance increase was observed until 100 nM of MSG concentration and reached saturation for a further rise in concentration. The MSG-added EIS spectra exhibited two distinct semi-circles. The characteristic semicircle at high frequencies having low RC values may describe the properties of the biosensor working electrode. In contrast, the second semi-circle with a quasi-linear response at low frequencies may be associated with the interfacial interaction of

MSG with antibodies at the electrode surface. It was observed that the second component has higher impedance and shifts towards lower frequencies with the addition of MSG. This observation is consistent with the DPV response.

Figure 5.7 A showed the DPV response of the biosensor working electrode in electrolyte without MSG. The addition of 100 nM of MSG in electrolytes showed a significant reduction of DPV peak current. To examine the usability of the developed biosensor for detecting MSG in real samples, freshly prepared tomato sauce was taken as a stock solution with 10 μ M of MSG and added to the electrolyte, making its final concentration 100 nM for DPV measurement.

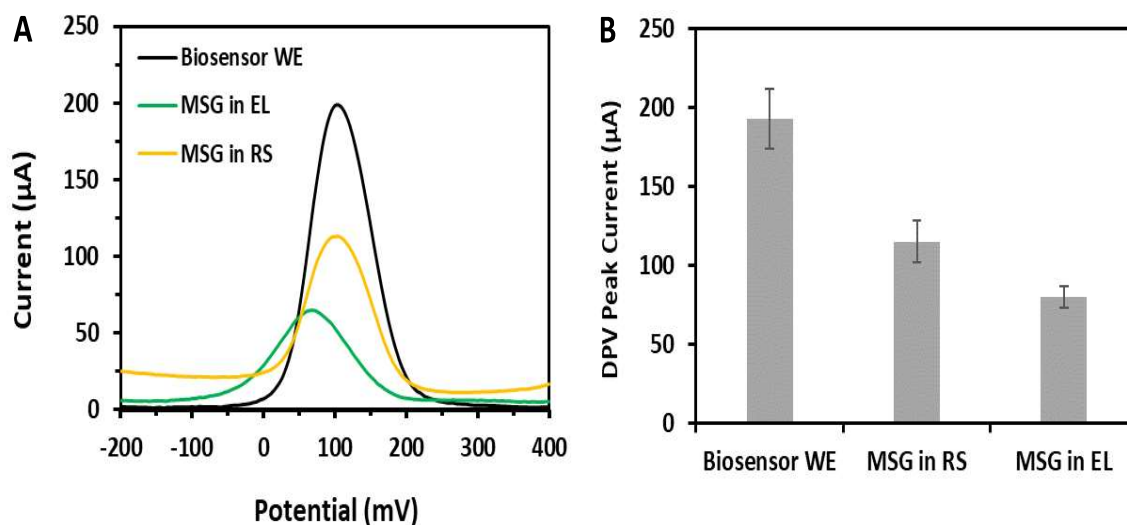


Figure 5.7: (A) DPV response of biosensor WE (antibody immobilized CS-GNP coated GCE) and 100 nM of MSG added to the electrolyte (MSG in EL), and 100 nM of MSG added to tomato sauce (MSG in RS). (B) Bar diagram representing a relative change in peak current in response to MSG in electrolyte and real sample.

The interaction of MSG from the real samples with antibodies at the surface of the biosensor working electrode showed a significant reduction in peak current. **Figure 5.7 B** shows a bar graph that represents the relative change in the DPV peak current. The MSG in the real

sample showed a 40% reduction in the DPV peak current, whereas a similar concentration of MSG in the standard electrolyte reduced the peak current by 58%. This difference may be expected due to the availability of MSG molecules in the electrolyte being relatively higher to interact with antibodies at the surface than MSG in a real sample. These initial studies are very encouraging, and further investigation of the different variations of MSG in real samples will be explored in the future.

Very high sensitivity towards MSG was observed due to unique characteristics of the working electrode platform developed by the coating of in-situ synthesized gold nanoparticles in chitosan. The current immunosensor showed the lowest range of detection, 0.1 nM, which is the highest sensitivity reported yet as per the available literature. This high sensitivity could be explained by the hypothesis that the working electrode developed with CS-GNP had shown enhancement in charge transportation, whereas functionalization by DC-NHS coupling allowed effective immobilization of antibodies at the CS-GNP surface. The reason for reduced sensitivity at higher concentrations of MSG is not well understood; however, it might be due to the accumulation of larger proportions of molecules at the surface of the electrode.

Previous studies had shown a relative comparison of MSG detection through an electrochemical biosensor [Table 5.1]. The lowest detection range value of the MSG reported to date was 50 nM using an electrochemical immunosensor [93]. The antibody-immobilized electrode showed exquisite sensitivity for detecting MSG in the range of nM to μ M.

5.4 Electrochemical Detection of MSG by LB film of PANI-TiO₂

Electrochemically polyaniline-titanium dioxide (PANI-TiO₂) was synthesized. Further, the electropolymerized PANI-TiO₂ nanocomposites were dissolved in a solution of N-methyl-2-pyrrolidone (NMP), and isopropanol for deposition of monolayer through the LB process and subsequent immobilization of monoclonal antibodies specific to L-glutamic acid was achieved. This may provide an advantage in increased conductivity of nanocomposites, higher charge transfer on the electrode surface, and uniform functionalization sites for binding of antibodies. The developed electrochemically active platforms were used for the quantification of monosodium L-glutamate (MSG) in electrolyte and tomato sauce.

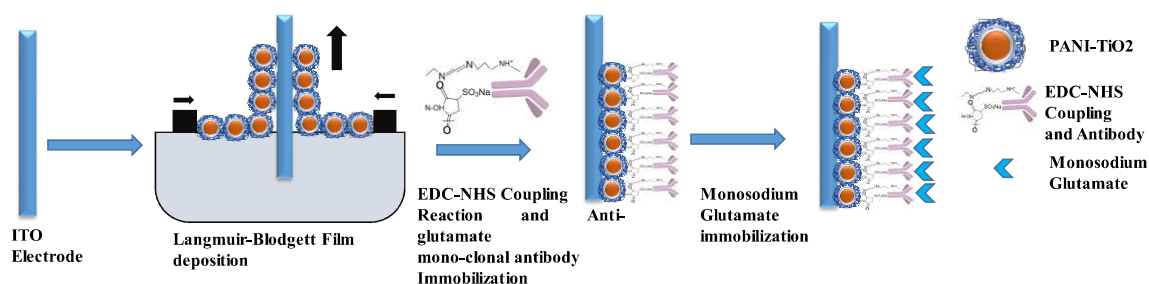


Figure 5.8: Schematic representation of immunosensor construction.

5.4.1 Preparation of Amperometry MSG Immunosensor

The following optimized procedure was used for the preparation of the glutamate biosensor. Firstly, the LB films of PANI-TiO₂ nanocomposite were deposited onto the ITO-coated glass and dried overnight at room temperature. 100 mM NHS and 400 mM EDC were prepared as stock solutions in 100 mM PBS and stored at 4° C. 10 μL of anti-glutamate monoclonal antibodies (1:100 dilution in PBS) were immobilized onto the functionalized electrode and kept undisturbed for 12 h at 4° C. The surface was rinsed thoroughly with PBS to remove the

unbound antibodies. Further, 50 μL of BSA was added onto the surface to block non-binding sites at the surface. The freshly prepared functionalized surface of PANI-TiO₂ was used for amperometry experiments. **Figure 5.8** shows the schematic representation of the immunosensor construction process.

5.4.2 Electrochemical Characterization

The electrochemical response of the ITO, LB film of PANI-TiO₂ on ITO, and antibody immobilized LB film of PANI-TiO₂ on ITO as the working electrode and BSA passivated antibodies immobilized PANI-TiO₂ electrode was assessed in 100 mM PBS containing 5 mM K₄[Fe(CN)₆] and 0.1M KCL (**Figure 5.9 A and B**). The potential range from -0.3 V to 0.8 V was used for measurements. Anodic (I_{pa}) and cathodic (I_{pc}) peak currents in the cyclic voltammetry response of the immunosensor were assessed.

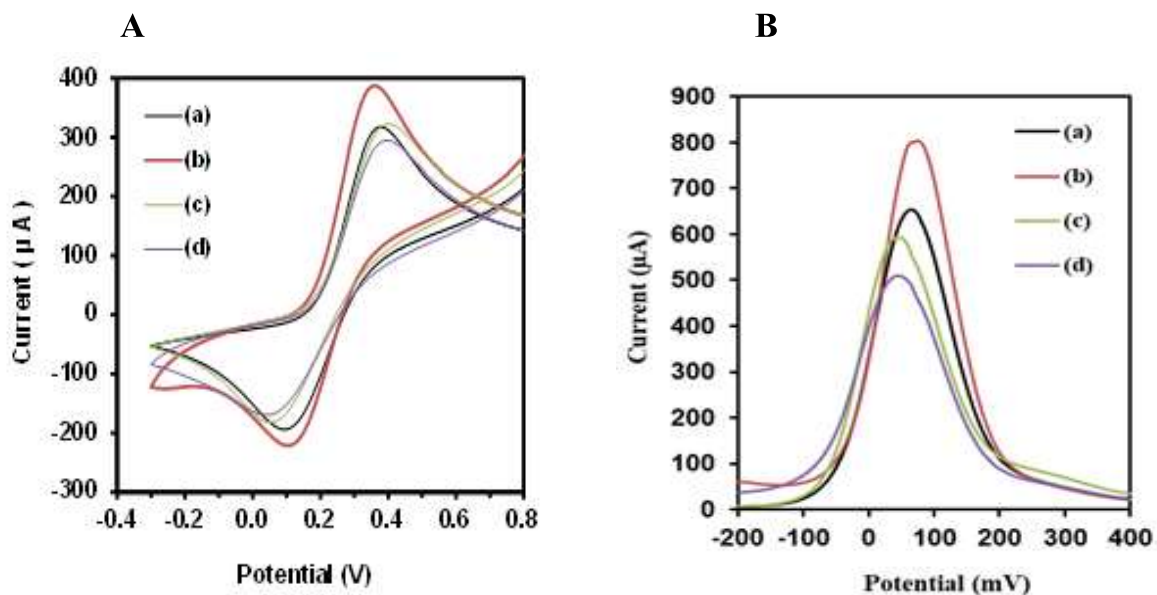


Figure 5.9: (A) CV and (B) DPV of different types of working electrodes. (a) ITO electrode, (b) PANI-TiO₂ LB film working electrode, (c) Rabbit anti-glutamate antibodies immobilized PANI-TiO₂ LB film working electrode, and (d) BSA passivated rabbit anti-glutamate antibody immobilized PANI-TiO₂ LB film working electrode.

I_{pc} and I_{pa} were increased from 318.2 μA to 387.3 μA and 194.5 μA to 221 μA after the deposition of LB film of PANI-TiO₂ on ITO. The conductivity enhancement was seen due to conducting nature of PANI-TiO₂, which may have helped in the fast electron transfer process between the electrolyte and the electrode. Further immobilization of antibodies on PANI-TiO₂ reduced both anodic and cathodic peak current from 387.3 μA to 322.5 μA and 221 μA to 182 μA . This may happen due to the non-conductive nature of antibodies; however, even after reduction, it retains peak current values similar to conducting ITO electrodes.

Cathodic ($E_{p,c}$) and anodic peak ($E_{p,a}$) potential were measured by CV response of different electrodes of ITO, PANI-TiO₂, antibodies immobilized PANI-TiO₂ and BSA passivated antibodies immobilized PANI-TiO₂ working electrodes. The difference in the potentials of both anodic and cathodic peaks ($\Delta E_p = E_{p,a} - E_{p,c}$) was calculated for these four different electrodes. The calculated ΔE_p for ITO, PANI-TiO₂, antibodies immobilized PANI-TiO₂, and BSA passivated antibodies similar for antibodies immobilized PANI-TiO₂ and BSA passivated antibodies immobilized PANI immobilized PANI-TiO₂ were 0.29 V, 0.26 V, 0.35 V, and 0.36 V, respectively. The ΔE_p remains the TiO₂ electrode whereas PANI-TiO₂ showed a decrease in ΔE_p , which confirmed fast kinetics of electron transfer on the electrode surface. Electron transfer on the electrode surface is inversely proportional to ΔE_p ($n \propto 1/\Delta E_p$) [43]. About 10 % of the decrease in the ΔE_p was observed, and a similar proportion of electrons was expected to increase in the process. This is expected due to the higher conductivity of aniline molecules in PANI and is supported by increased peak currents of both oxidation and reduction processes.

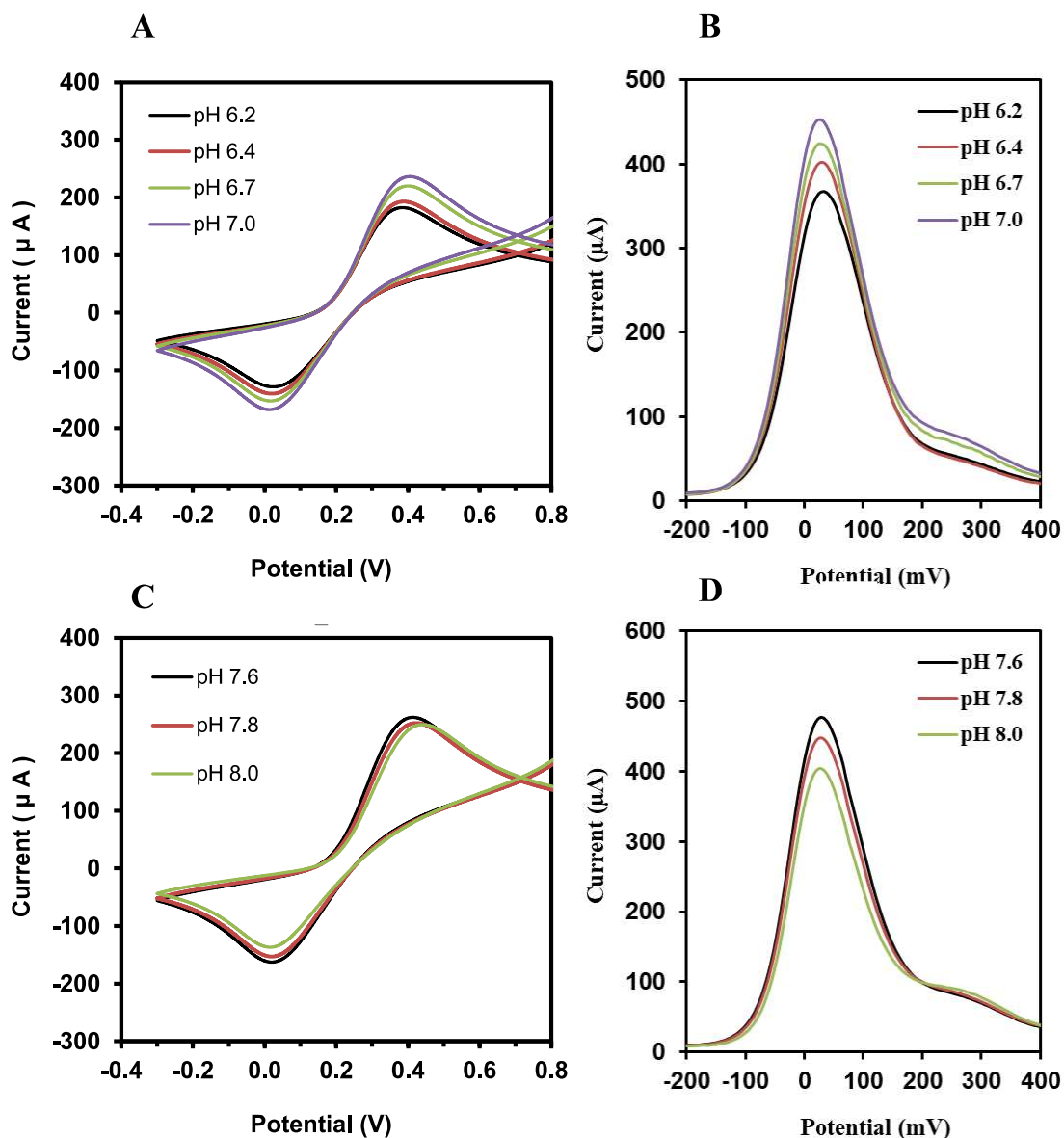


Figure 5.10: (A) CV and (B) DPV of PANI-TiO₂ immunosensor at various pH in acidic range and (C) CV and (D) DPV of PANI-TiO₂ immunosensor at various pH in basic range.

Further immobilization of antibodies on the PANI-TiO₂ surface showed an increase in ΔE_p by 35%, resulting in a decrease in a similar proportion of electron transportation. The observations are consistent with the expected outcomes as the non-conducting nature of antibodies at the electron's surface reduces its diffusion from the electrolyte to the working electrode surface.

DPV response of ITO and different platforms (PANI-TiO₂, Antibody-PANI-TiO₂, and BSA-antibody-PANI-TiO₂) on ITO electrodes was carried out in the same electrolyte. Peak current (I_p) was increased from 654 μA to 804 μA after LB film deposition of PANI-TiO₂ on the ITO electrode. The enhanced conductivity of PANI-TiO₂ may be due to the conductive nature of aniline molecules. Rabbit anti-glutamate antibodies immobilized PANI-TiO₂ surface result showed a decrease of I_p from 804 μA to 594 μA , similar to ITO response. Further passivation of the surface by BSA was achieved to minimize the direct interaction of electrolytes at the working electrode surface.

The antibody immobilized at the surface of PANI-TiO₂ may respond differently to a change in the pH of the electrolyte solution. CV has been recorded on immunosensor working electrodes at pH variation in acidic (pH from 6.2 to 7) and basic (7.6 to 8) ranges and the results are shown in **Figure 5.10 (A, C)**. I_{pc} and I_{pa} were decreased from 236.3 μA to 182.5 μA and 168 μA to 128.5 μA with the reduction in pH from 7.0 to 6.2 on antibodies immobilized LB film of PANI-TiO₂ on ITO. The ΔE_p was decreased by 8 % with a decrease in pH values in the acidic region, indicating an increase in electron transportation. This could be due to the polarization of antibodies' surfaces while the number of charged particles in electrolytes increased with pH reduction from its neutral value. Similar results were observed for the increase in pH in the basic region. I_{pc} and I_{pa} were decreased from 262 μA to 250 μA and 163 μA to 137 μA , respectively, with an increase in pH from 7.6 to 8.0 on antibodies immobilized LB film of PANI-TiO₂ on ITO. The ΔE_p was increased by 7 %, increasing the pH values in the basic region, indicating a decrease in electron transportation. This observation is consistent with acidic pH variation observations, where a relative increase in the number of electrons on the electrode surface was observed. In contrast, the number of

charged particles in electrolytes increased with pH reduction from its neutral value. Whereas with the increase in basic pH, the charge polarity in the electrolyte may be reversed, and a decrease in a similar proportion of charged particles was observed on the electrode surface. DPV response of BSA-antibody-PANI-TiO₂ on the ITO electrode at various pH levels in acidic and basic conditions was also measured, and the results are shown in **Figure 5.10 (B, D)**. Peak current (I_p) was decreased from 453 μ A to 368 μ A with a decrease in pH from 7 to 6. Similarly, in the basic region, the pH increases from 7.6 to 8, reducing the peak current from 476 μ A to 404 μ A. The excess concentration of charge in the electrolyte might polarize the antibodies at the surface of the working electrode, hence decreasing the peak current. Therefore, the experimental observations indicated the highest current for the pH range (7.2 to 7.4), known as an “Optimum physiological condition” This is also a safe range for glutamate, which can be protonated or de-protonated in acidic and basic conditions wherein glutamate gets converted to glutamic acid. Thus, it could not interact with the antibody [93]. While in basic condition, hydroxyl ion as cationic sites on the functionalized electrode surface results in interference which causes a change in potential.

The interaction of the BSA passivated antibody immobilized PANI-TiO₂ on the ITO working electrode at different MSG concentrations was assessed. Gradually the MSG concentration was increased, and at every step, CV response was recorded, and results are shown in **Figure 5.11 A**.

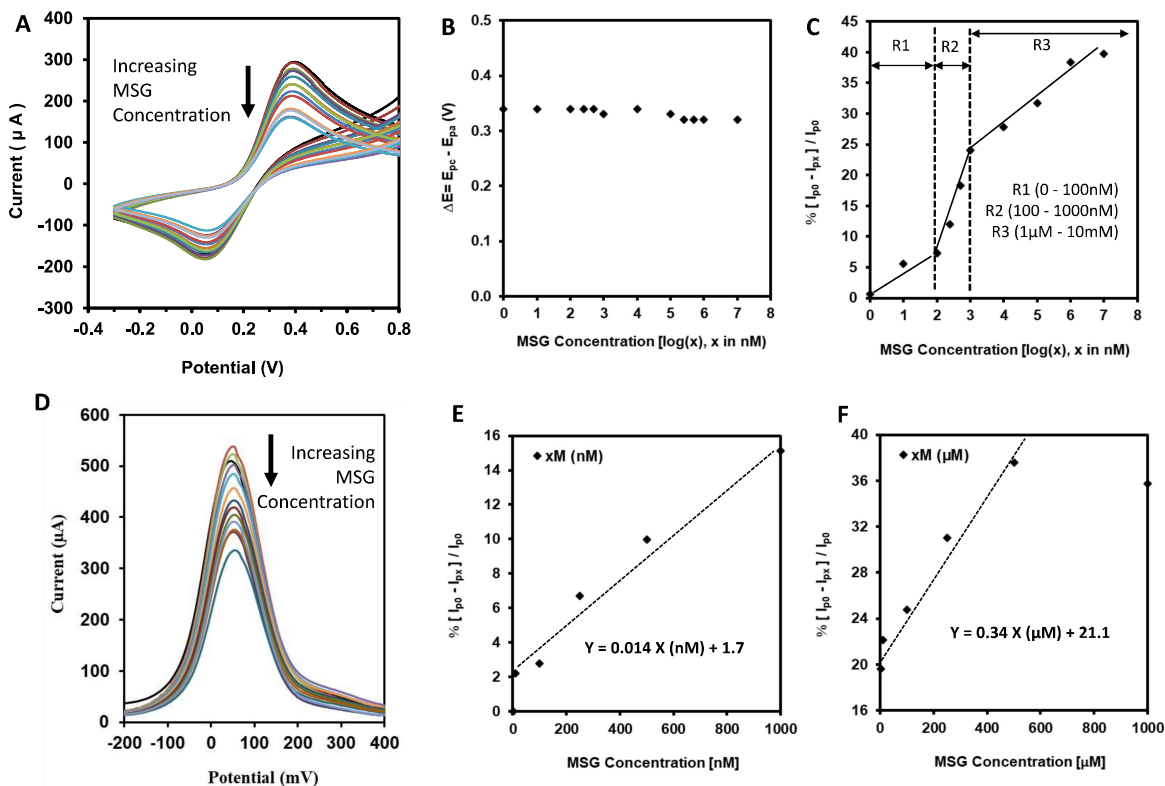


Figure 5.11: (A) CV response of PANI-TiO₂ immunosensor working electrode with different concentrations of MSG, (B) Relative change in peak potential with MSG concentrations, (C) Relative change in peak current with MSG concentrations, (D) DPV response of CS-GNP-IgG working electrode with different concentrations of MSG. (E) Relative change in % peak current with MSG concentrations varying in nM concentration, and (F) Relative change in % peak current with MSG concentrations varying in μM concentration.

The ΔE_p remains constant with increasing concentrations of MSG. Anodic (I_{pa}) and cathodic (I_{ca}) peak currents response of working electrodes with and without MSG in electrolytes were assessed and compared. The value of I_{pa} was measured, and the % relative change $[(I_{p_0} - I_{p_x})/I_{p_0}]$, where I_{p_0} is peak current without MSG and I_{p_x} is peak current at 'x' nM of MSG, was plotted with a wide range of MSG variation in the electrolyte. Initially, at a scarce concentration of MSG (R1 = 0 to 100 nM), a straight-line response was observed; the second response was for R2 from 100 nM to 1000 nM, and finally, the third region, R3, from 1 μM

to 10 mM. The results suggested that with precise control of surface molecular layer properties, a wide range of MSG detection was possible with different calibration regions. DPV results in **Figure 5.11** revealed that peak current is inversely proportional to the increase in MSG concentration. This may be due to the formation of anti-glutamate antibodies and L-glutamate antigen complex, which plays an important role in the selective detection of MSG. This complex system creates a diffusion layer that blocks the transfer of ions between the solution and electrode surface. As a result, active sites for electron transfer were reduced, and the working electrode platform's conductivity was decreased with an increase in MSG concentration. The % relative change in peak current with MSG concentration was also consistent with CV measurement, as shown in **Figure 5.11 C**. The working electrode developed with PANI-TiO₂ showed enhancement in the charge transportation, whereas functional group presence allowed effective immobilization of antibodies at the surface. The antibodies immobilized electrode showed exquisite sensitivity for detecting MSG in the range of nM to mM.

DPV was used to obtain the current-voltage characteristics of the immunosensor prepared using PANI-TiO₂ LB films at different concentrations of MSG added in tomato sauce, and the relative change in peak current was recorded. DPV measurements were carried out by placing antibodies-immobilized working electrodes in 10 ml of phosphate buffer (pH 7.0), having MSG added to tomato sauce. The solution was stirred for 30 s before taking each

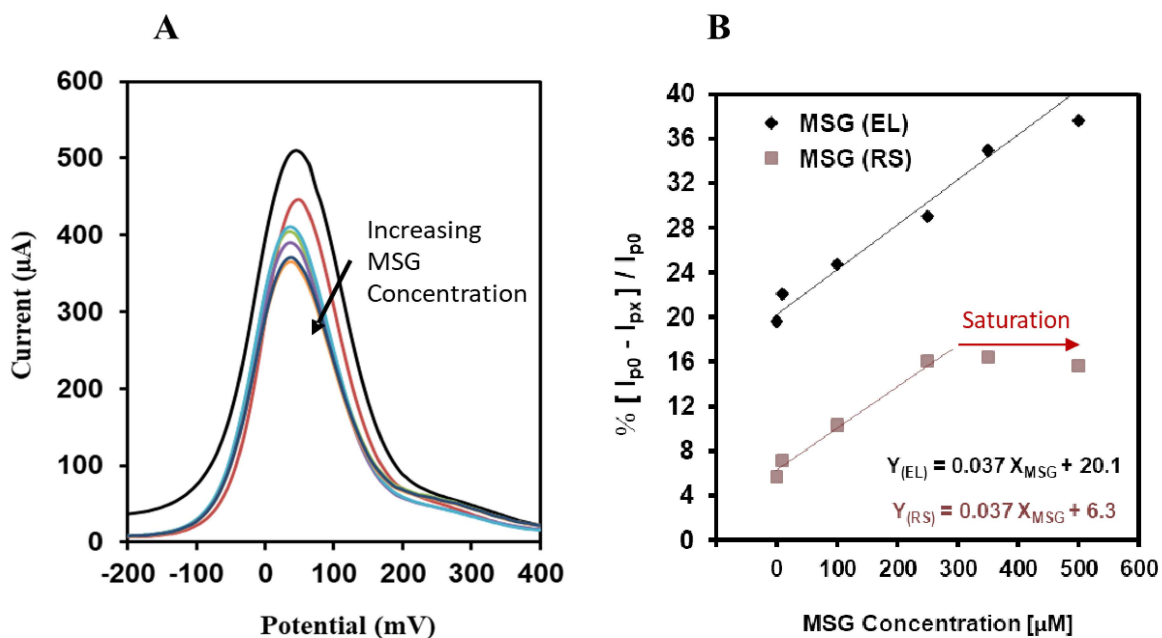


Figure 5.12: (A) DPV response of PANI-TiO₂ immunosensor working electrode without and with tomato sauce at different concentrations of MSG, (B) Immunosenor response for quantification of MSG concentrations where MSG (EL) represents MSG in standard electrolyte and MSG (RS) represents MSG in tomato sauce.

measurement. The MSG concentrations in tomato sauce were increased by adding MSG with gradual increments in the range of 10 µM to 500 µM in buffer solution, and the results are shown in **Figure 5.12 A**. Platinum wire, and Ag/AgCl was used as counter and reference electrodes, respectively. **Figure 5.12 B** showed a quantitative analysis of MSG detection in terms of percentage relative changes $\Delta I = [100\{(I_{P0} - I_{PX})/I_{P0}\}]$ in peak current for the PANI-TiO₂ electrode. I_{P0} and I_{PX} are peak currents measured in DPV without the use of MSG and with ‘X’ molar concentration of MSG, respectively.

Linear response for detecting MSG was observed, which was expressed as $\Delta I_{RS} = 0.037 X_{MSG} + 6.3$, where X_{MSG} is the concentration of MSG in tomato sauce (described as a real sample) added to electrolyte during the measurement. The detection sensitivity was

calculated from the linear response slope in the current variation with increasing MSG concentrations, which was 37 mA/nM. The detection range for the real sample tested was from 1 μM to 250 μM concentration. A quantitative analysis of MSG detection in terms of percentage relative changes $\Delta I = [100\{(I_{PO} - I_{PX})/I_{PO}\}]$ in peak current for PANI-TiO₂ electrode was also calculated for the use of MSG in the standard electrolyte from the DPV measurements, as shown in **Figure 5.12 B**. These were described as MSG in the electrolyte MSG (EL). I_{PO} and I_{PX} are peak currents measured in DPV without using MSG and with 'X' molar concentration of MSG, respectively, by adding MSG to the standard electrolyte. Linear response for detecting MSG was observed, which was expressed as $\Delta I_{EL} = 0.037 X_{MSG} + 20.1$, where X_{MSG} was the concentration of MSG in the standard electrolyte (described as electrolyte) during the measurement.

The detection sensitivity was calculated from the linear response slope in the current variation with increasing MSG concentrations, which was 37 mA/nM. The range of detection of MSG was tested in the standard electrolyte from 1 μM to 500 μM concentration. The detection sensitivity remained unchanged for both tomato sauce samples and standard electrolytes. However, the detection range for MSG in standard electrolytes showed linear response for an extended range, whereas real samples showed saturation at 250 μM MSG concentration in the current study. The working electrode developed with PANI-TiO₂ showed enhancement in the charge transportation, whereas functional group presence allowed effective immobilization of antibodies at the surface. The antibodies immobilized electrode showed exquisite sensitivity and consistency for the detection of MSG. **Table 5.1** summarizes the detection sensitivity of MSG obtained with different biosensor platforms prepared by different methods.

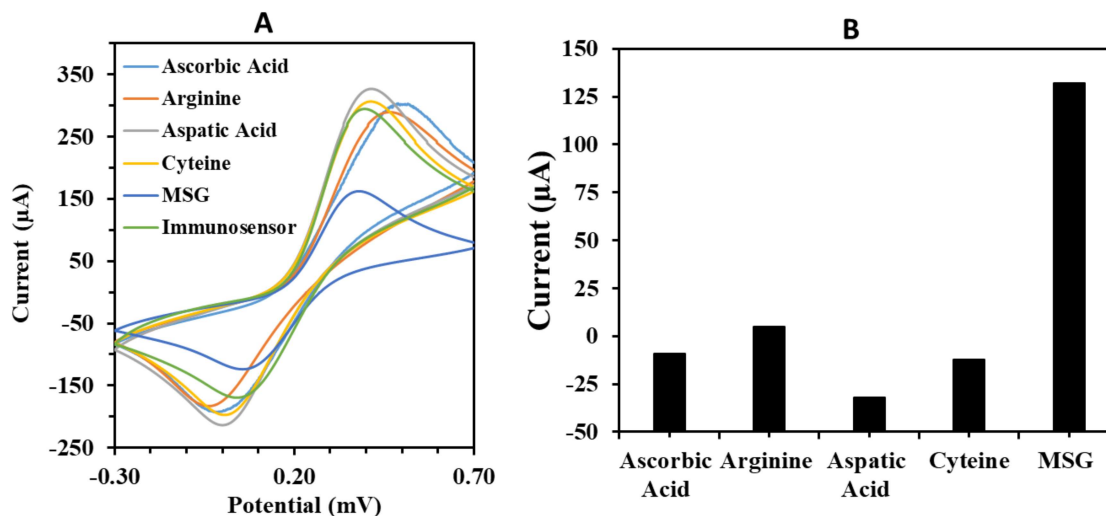


Figure 5.13: (A) CV response of immunosensor with different analytes, (CV response of black- immunosensors, green- with MSG and red- with different analytes), and (B) Relative change in peak current of CV response while different analytes added into the electrolyte, (a) ascorbic acid, (b) arginine (c) aspartic acid (d) cysteine and (e) MSG.

The specificity of the developed biosensor was also examined with the use of other analytes (ascorbic acid, arginine, aspartic acid, and cysteine) in the electrolytes. **Figure 5.13 A** shows the CV response of the biosensor platform with the use of similar molar concentrations of theirs in the electrolyte. It is clearly evident that there has not been a significant change in the peak current of CV response acquired with the use of different analytes. The addition of a similar molar concentration of MSG in the electrolyte had substantially reduced the peak current in CV response. Relative change in the oxidation peak current during measuring CV response was calculated for all different analytes, and results are plotted in **Figure 5.13 B**. These results confirm the advantage of using nanocomposites having both biocompatible and conducting nature for making biosensors platforms by depositing monolayers for effectively quantifying analytes in the electrolyte with higher sensitivities and selectively.

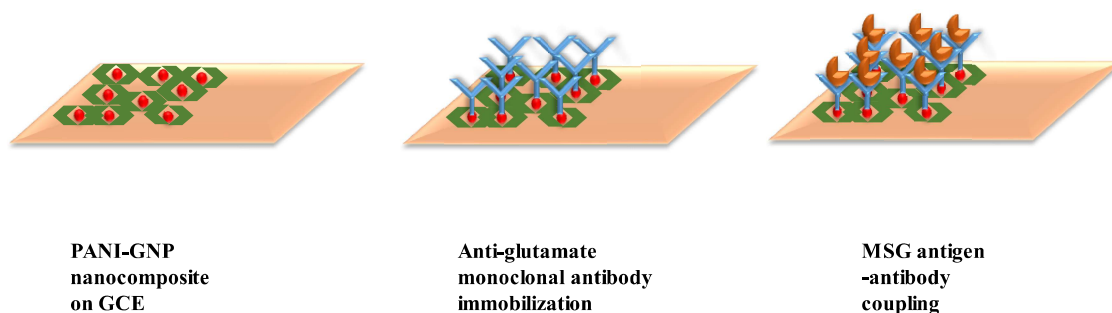


Figure 5.14: (A) Schematic representation of electrochemical Immunosensor development.

5.5 Electrochemical Detection of MSG by LB film of PANI- GNP

We have formulated a unique design where a positively charged monomer of a conductive polymer has been electro-polymerized on the surface of negatively charged metallic nanoparticles. The conductive polymer matrix facilitates the stacking of the nanoparticles and prevents their aggregation without decreasing their conductivity. Due to electrostatic forces of attraction, a stable nanocomposite of PANI/GNP has been obtained; an absence of hydroxyl group in the C1s XPS analysis confirmed relative hydrophobic characteristics of the synthesized nanocomposite, which enabled their deposition as a monolayer at the water-air interface [220]. GNPs were chosen due to their exceptional conductivity and high stability over a wide range of pH and temperatures. The LB film of PANI-GNP nanocomposite results in the amplification of conductivity and has been used as a working electrode in developing an electrochemical immunosensor to quantify MSG.

5.5.1 Preparation of Amperometric Mono Sodium Glutamate Biosensor

The following optimized procedure was used to prepare the MSG biosensor: First, the LB films of PANI-GNP nanocomposite were deposited onto the ITO-coated glass and dried overnight at room temperature. The very next day, 100 mM NHS and 400 mM EDC were prepared as stock solutions in 100 mM PBS (pH 7.4) and stored at 4°C. Further EDC-NHS

mixture was prepared by mixing NHS and EDC in a 1:1 ratio. 50 μL of EDC-NHS mixture was cast onto the LB film of PANI-GNP and dried for two hours. After drying, 10 μL of anti-glutamate monoclonal antibody (1:100 dilution) in PBS (pH 7.0) was immobilized onto functionalized LB film of PANI-GNP electrode and kept undisturbed for 12 h at 4°C. After that, 50 μL of Bovine Serum Albumin (BSA) was cast onto the electrode surface. This immunosensor was stored at 9°C before subjecting to electrochemistry experiments. The developed immunosensor was rinsed thoroughly with PBS to remove the unbound molecules from the electrode surface.

5.5.2 Electrochemical Characterization

The surface morphology of the LB film surface on ITO was examined along with different successive modifications in it due to antibody immobilization and BSA passivation for developing a biosensor to detect MSG, as shown in the schematic diagram (**Figure 5.14**), and the corresponding surface morphologic changes were indicated. CV of bare ITO, LB film of PANI-GNP nanocomposite (PANI-GNP/ITO), anti-glutamate antibody immobilized on LB film of PANI-GNP nanocomposite (Anti-Glu/ PANI-GNP/ITO), and after BSA casting to passivate electrode surface (BSA/Anti-Glu/ PANI-GNP/ITO), was carried out in 100 mM PBS solution having pH value 7.4 containing 5 mM $\text{K}_4[\text{Fe}(\text{CN})_6]$ and 0.1M KCL. Voltage was cycled between - 0.3 to 0.7 V.

Figure 5.15 A reveals an increase (from $\sim 318 \mu\text{A}$ to $\sim 350\mu\text{A}$) in anodic peak current (I_{pa}) and a decrease ($\sim -195\mu\text{A}$ to $\sim -171 \mu\text{A}$) in cathodic (I_{pc}) peak currents in the negative current range after LB film of PANI-GNP deposited on ITO. This change in I_{pa} and I_{pc} was 10% and 14%, respectively, which could be associated with a positive surface charge on the surface of the PANI-GNP nanocomposite. The difference in the potential of both

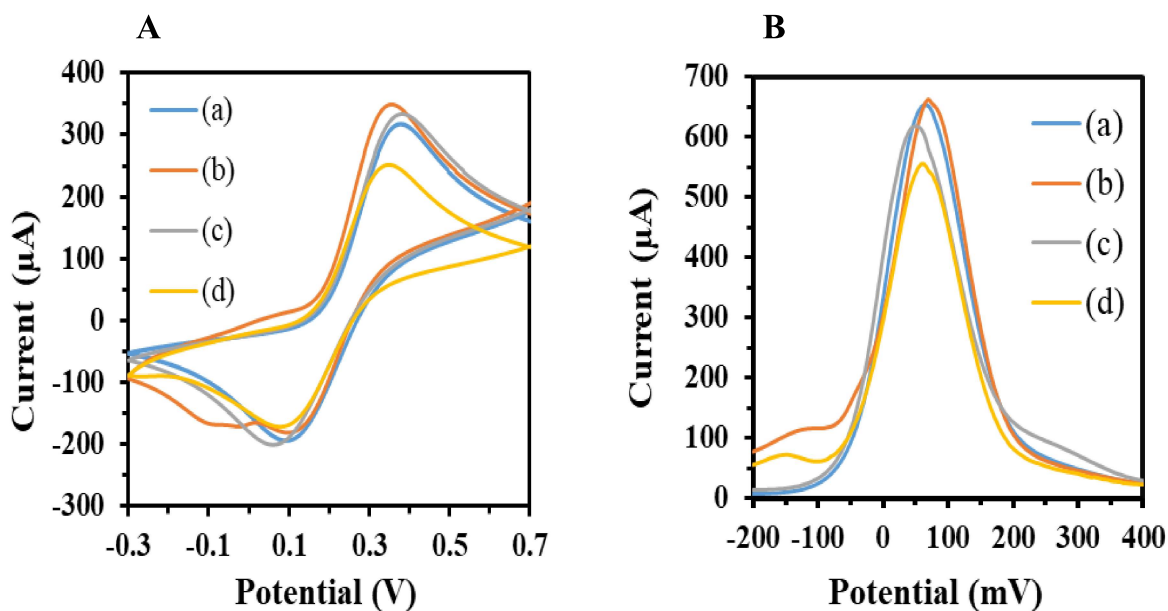


Figure 5.15: (A) CV and (B) DPV of different types of working electrodes. (a) ITO electrode, (b) PANI-GNP LB film working electrode, (c) Rabbit anti-glutamate antibodies immobilized PANI-GNP LB film working electrode, and (d) BSA passivated rabbit anti-glutamate antibody immobilized PANI-GNP LB film working electrode.

anodic and cathodic peaks were reduced to 0.03 V in PANI-GNP. Electron transfer on the electrode surface is inversely proportional to change in ΔE_p ($n \propto 1/\Delta E_p$) [57].

Thus, this decrease in peak potential of LB film of PANI-GNP to bare ITO confirms the fast kinetics of electron transfer on the electrode surface. Rabbit anti-glutamate antibodies were immobilized onto PANI-GNP film-coated surface. After immobilization of the antibodies, the I_{pa} decreases from $\sim 350 \mu A$ to $\sim 333 \mu A$, and I_{pc} from $\sim -171 \mu A$ to $\sim -201 \mu A$, but peak potential increases for both anodic and cathodic peaks from 0.03V to 0.04V. This 5% and 15% decrease in I_{pa} and I_{pc} , respectively, may happen due to the non-conductive nature of antibodies; however, even after reduction, it retains peak current values more than the bare ITO electrodes. Bovine serum albumin (BSA) is commonly used for passivating the surface,

covering unwanted binding sites, and reducing the speedy and inefficient electron transfer between the electrolyte and working electrode. BSA blocked the PANI-GNP surface where

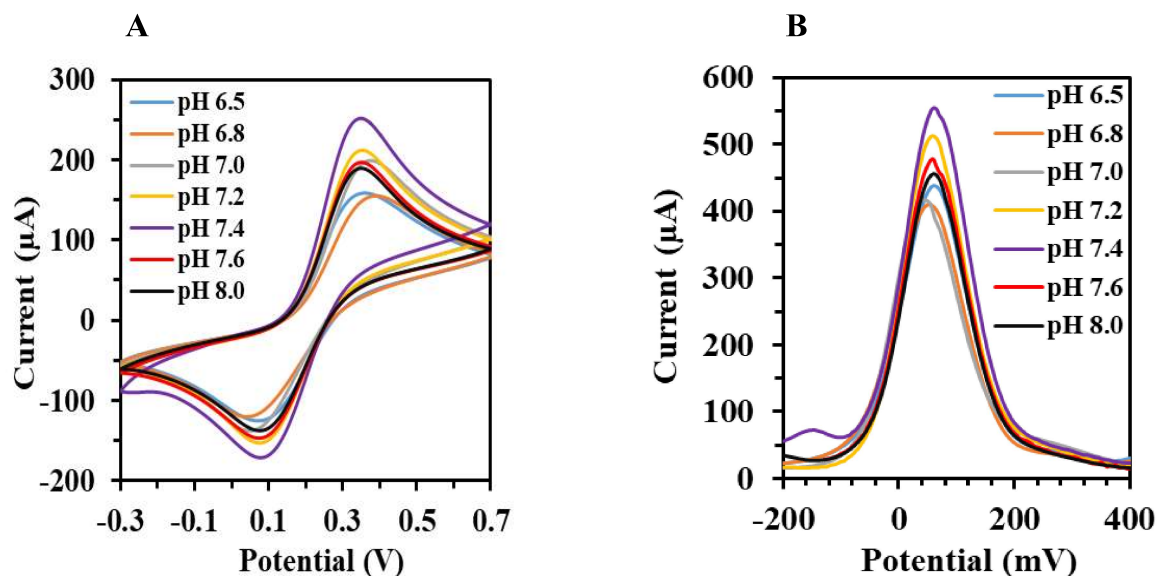


Figure 5.16: (A) DPV of PANI-GNP immunosensor at different pH ranges.

antibodies were not bound, preventing direct electron transfer at the working electrode surface. Thus, a further decrease was observed in I_{pa} from $\sim 333 \mu\text{A}$ to $\sim 252 \mu\text{A}$ and I_{pc} from $\sim -201 \mu\text{A}$ to $\sim -172 \mu\text{A}$. This affirms our notion of efficient covering of unwanted open binding sites by BSA and the modified electrode's suitability for immune-sensing applications. The difference in the potentials of both anodic and cathodic peaks after BSA passivated antibodies immobilized PANI-GNP were increased by 0.03 V and 0.01 V, respectively. The non-conductive nature of antibodies and BSA plays a pivotal role in this potential shift. CV study shows that the antibody is effectively immobilized onto the LB film of the PANI-GNP nanocomposite surface and is covered by the BSA. To confirm the above results further, we have conducted the DPV study. DPV response of ITO and different platforms (modified with LB film of PANI-GNP nanocomposite (PANI-

GNP/ITO), anti-glutamate antibody immobilized LB film of PANI-GNP nanocomposite (Anti-Glu/ PANI-GNP/ITO), and after BSA casting (BSA/Anti-Glu/ PANI-GNP/ITO) were carried out in the same electrolyte. DPV is an essential tool in electrochemistry, where the measuring peak current is directly proportional to the conductivity of the electrode. **Figure 5.16 B:** Peak current (I_p) was increased by $\sim 8 \mu\text{A}$ after LB film deposition of PANI-GNP on the ITO electrode. However, after immobilizing antibodies and BSA, the peak current decreases by $\sim 44 \mu\text{A}$ and $\sim 63 \mu\text{A}$, respectively. Thus, both electrochemical tools confirm the effective immobilization of antibodies onto the LB film of the PANI-GNP surface and ensure good electrical conductivity and high surface area of the immunosensor.

CV and DPV response of immunosensor (BSA/Anti-Glu/ PANI-GNP/ITO) on ITO electrode was recorded at varying pH ranges, i.e., 6.5 to 8.0 conditions, and the results have been compiled and shown in **Figure 5.16 A and B**. Peak current (I_p) was decreased from $\sim 555 \mu\text{A}$ to $\sim 440 \mu\text{A}$ with a decrease in pH from 7.4 to 6.5. Similarly, in the basic region, the pH increases from 7.4 to 8, reducing the peak current from $\sim 555 \mu\text{A}$ to $\sim 456 \mu\text{A}$. The excess concentration of charge in the electrolyte might polarize the antibodies at the surface of the working electrode, hence decreasing the peak current. Therefore, the experimental observations indicate the highest current for the pH value of 7.4, known as an "Optimum physiological condition" This is also safe for glutamate, which may be protonated or de-protonated in acidic and basic conditions, wherein glutamate gets converted to glutamic acid. Thus, it could not interact with the antibody. While in basic conditions, hydroxyl ion acts as a cationic site on the functionalized electrode surface, causing interference, which results in a change in potential.

Relative change in biosensor conductivity was measured to determine the sensitivity and detection range for MSG in an electrolyte solution. Gradually the MSG concentration was increased from 1 nM to 10 mM step by step in the electrolyte, and at each step, CV and DPV responses were measured. **Figure 5.17** A shows CV response, and both anodic (I_{pa}) and

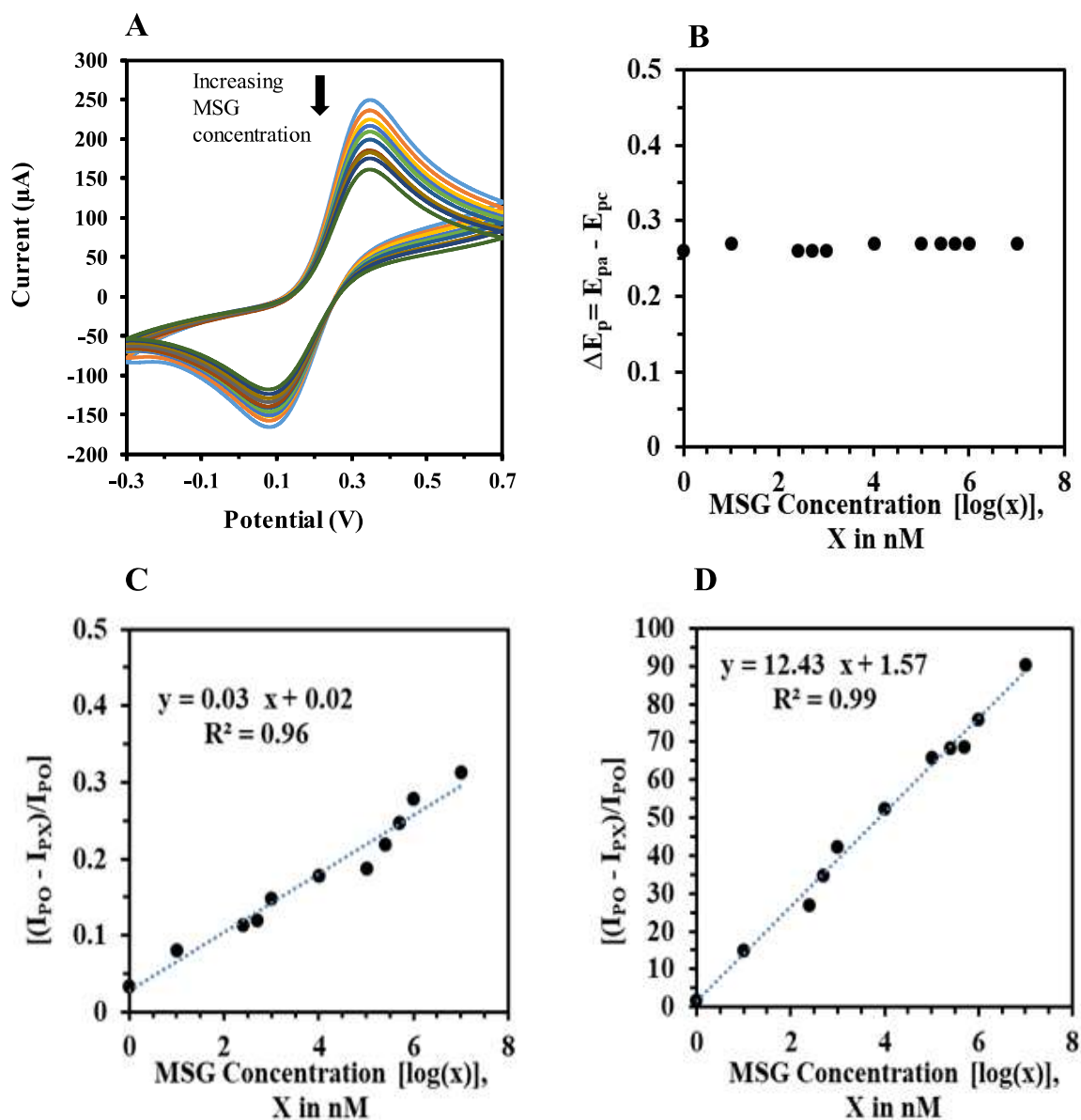


Figure 5.17: (A) CV response of PANI-GNP immunosensor working electrode with different concentrations of MSG, (B) Relative change in peak potential with MSG concentrations, (C) Relative change in cathodic peak current with MSG concentrations, and (D) Relative change in anodic peak current with MSG concentrations.

cathodic (I_{ca}) peak currents were measured at the biosensor surface with and without the addition of MSG at various concentrations in the electrolyte. The anodic peak current of the biosensor working electrode was $\sim 252 \mu\text{A}$ without MSG and $\sim 250 \mu\text{A}$ with the addition of 1 nM MSG. A decrease in the value of I_{pa} and I_{ca} was observed from $\sim 250 \mu\text{A}$ to $\sim 183 \mu\text{A}$ and $\sim 166 \mu\text{A}$ to $\sim 129 \mu\text{A}$, respectively, with an increase in MSG concentration from 1 nM to 10 mM. The ΔE_p remains constant with increasing concentrations of MSG (**Figure 5.17 B**). The relative change in both anodic and cathodic peak currents was measured at various concentrations of MSG, and the results are shown in **Figures 5.17 C**, and **5.17 D**. Both the peak currents are inversely proportional to the MSG concentration in the electrolyte. This relationship between peak current and MSG concentration happens due to antibody-antigen interaction, which plays an essential role in the selective quantification of MSG in the electrolyte by the use of a developed biosensor platform. GNP in PANI enables high electrical conductivity, high surface area, and the binding site for the anti-glutamate monoclonal antibody. In contrast, the PANI provides good adhesion, permeability, and electrical conductivity between the gold nanoparticle and the ITO surface. Due to the hydrophobic nature of PANI, it provides permeability in the reaction mixture and facilitates the electron transfer between the electrode and electrolyte solution. Thus, the combination of a PANI-GNP nanocomposite provides with excellent electrochemical properties. Therefore, we were able to detect MSG small concentration (1 nM) with a wide detection range due to the increased conductivity of PANI-GNP nanocomposite with a better choice for antibody functionalization due to the availability of amine groups across the surface. The hypothesis for the detection of MSG was based on as we add MSG to the solution, anti-glutamate antibodies interact with the MSG molecule forming an antigen-antibody complex. This

complex system makes a diffusion layer that blocks the transfer of $K_4[Fe(CN)_6]$ ion between the solution and electrode surface, hence reducing the active site for electron transfer and effective area.

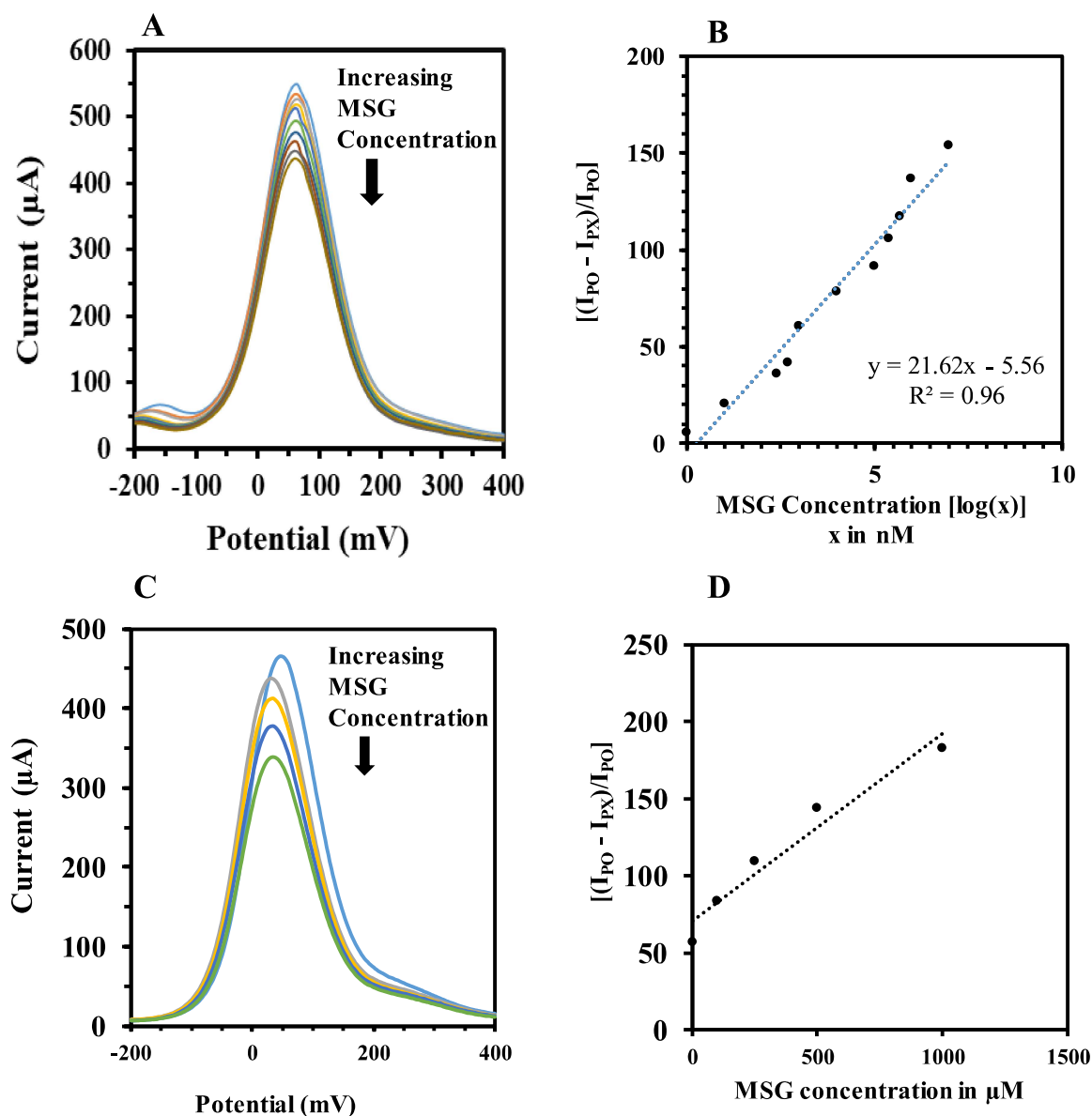


Figure 5.18: (A) DPV response of PANI-GNP immunosensor with different concentrations of MSG in the electrolyte, (B) Relative change in % peak current with MSG concentrations in the electrolyte, (C) DPV response of PANI-GNP immunosensor with different concentrations of MSG in the real sample and (D) Relative change in % peak current with MSG concentrations in the real sample.

DPV results in **Figure 5.18 A** reveal that the peak current decreases with an increase in MSG concentration in the electrolyte. The % relative change in peak current with MSG concentration was consistent with CV measurement, as shown in **Figure 5.17 A**. The

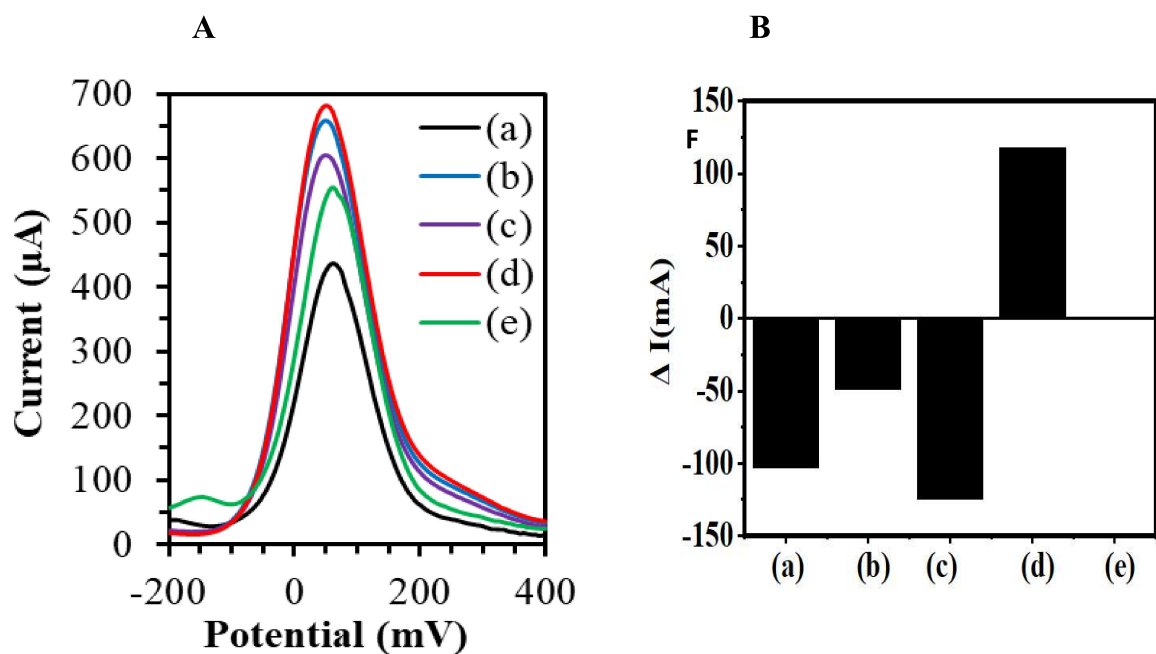


Figure 5.19: (A) DPV response of PANI-GNP immunosensor with different analytes (a) 500 μM MSG, (b) 500 μM Arginine, (c) 500 μM Aspartic acid, (d) 500 μM Cysteine, (e) without MSG. (B) Relative change in peak current with immunosensor.

antibodies immobilized immunosensor showed exquisite sensitivity for detecting MSG in the nM to mM range. PANI-GNP LB film-based immunosensor was studied with DPV to obtain current-voltage characteristics of different concentrations of MSG added to the electrolyte. The relative change in peak current was recorded. These results are shown in **Figure 5.18 B**. DPV measurements were carried out by placing the immunosensor in 10 ml of phosphate buffer (pH 7.0), with MSG added to the tomato sauce sample (**Figure 5.18 C**). The MSG concentrations in the sample were increased by adding it in gradual increments from 1 μM to 1 mM. **Figure 5.18 D** showed the quantitative analysis of MSG

detection in terms of percentage relative changes $\Delta I = [100 \{(I_{PO} - I_{PX})/I_{PO}\}]$ in peak current for the PANI-GNP electrode. Linear response for detecting MSG was observed; the detection range for the real sample tested was from 1 μ M to 1 mM concentration.

However, the detection range for MSG in standard electrolytes showed linear response for an extended range, i.e., 1 nM to 10 mM. In contrast, tomato sauce samples showed saturation at 1 mM MSG concentration in the current study. **Figure 5.19 A** presented the DPV quantitative analysis of PANI-GNP immunosensor with different analytes, i.e., 500 μ M MSG, 500 μ M Arginine, 500 μ M Aspartic acid, 500 μ M Cysteine, without MSG.

Figure 5.19 B represents the relative change in the peak current of different analytes compared to immunosensor without MSG. These results show that the PANI-GNP immunosensor is not sensitive to similar analytes like MSG as there is no decrease in current. The working electrode developed with PANI-GNP exhibits enhanced charge transportation, whereas functional group presence allows effective immobilization of antibodies at the surface. The antibodies immobilized electrode shows outstanding sensitivity and consistency for the detection of MSG.